

Full Length Research Paper

Investigation of drug delivery on anticancer drug by SWCNT with theoretical studies

M. Monajjemi^{1*}, A. Sobhanmanesh¹ and F. Mollaamin²

¹Department of Chemistry, Science and Research Branch, Islamic Azad University, Tehran, Iran.

²Department of Chemistry, Qom Branch, Islamic Azad University, Qom, Iran.

Accepted 6 September, 2011

The interaction of anticancer drug $\text{Sn}(\text{CH}_3)_2(\text{N-acetyl-L-cysteinate})$, that is called (N-acetyl-L-cysteinato-O,S) dimethyl tin(IV), with single walled carbon nanotube (SWCNT) is investigated by Quantum chemical *ab initio* calculations at HF/(LanL2DZ+STO-3G) and HF/(LanL2DZ+6-31G) levels in gas phase and solution. The solvent effect is taken into account via the self-consistent reaction field (SCRF) method. Carbon nanotubes can act as a suitable drug delivery vehicle for internalization, transportation and translocation of $\text{Sn}(\text{CH}_3)_2(\text{N-acetyl-L-cysteinate})$ within biological systems. Thermodynamical analysis indicates that the relative energies (ΔE), enthalpies (ΔH) and free Gibbs energies (ΔG) are negative for $\text{Sn}(\text{CH}_3)_2(\text{N-acetyl-L-cysteinate})$ -CNT system, but the calculated entropies (ΔS) are positive, suggesting thermodynamic favorability for covalent attachment of $\text{Sn}(\text{CH}_3)_2(\text{N-acetyl-L-cysteinate})$ into carbon nanotube. Also, the results show that with increasing dielectric constant of solvent, the stability of $\text{Sn}(\text{CH}_3)_2(\text{N-acetyl-L-cysteinate})$ -CNT complex decreases. Furthermore, anisotropic chemical shift tensor ($\Delta\sigma$), total atomic charge and asymmetry parameter (η) have been calculated using the gauge-including atomic orbital (GIAO) method, results being compared with CGST data. From the nuclear magnetic resonance (NMR) calculations, it can be seen that the NMR ($\Delta\sigma$, η) parameters at the sites of nitrogen and oxygen, as well as C-2 and C-3 nuclei are significantly influenced by intermolecular hydrogen-bonding interactions, but the quantity at the site of S-27 is influenced by nonspecific solute-solvent interaction, such as polarisability/polarity.

Key words: $\text{Sn}(\text{CH}_3)_2(\text{N-acetyl-L-cysteinate})$, nuclear magnetic resonance (NMR) parameters, single walled nanotube (SWNT), solvent.

INTRODUCTION

The chemistry of organotin(IV)s has witnessed an increased interest during the last fifty years, owing to their potential biological and industrial applications. However, some organotin(IV) compounds, which were originally modeled on the first tumor-active platinum compound, cisplatin (Barnard, 1989), have also found their place among a class of non-platinum chemotherapeutic metallopharmaceuticals exhibiting good antitumor activity (Clarke et al., 1999; Nath et al., 2001). In this context, diorganotin(IV) derivatives and mainly those of dialkyltin(IV) complexes from amino acids ligand are known to possess antimicrobial (Plesch et al., 1988), anti-malarial (Goldberg et al., 1997), antiproliferative (Kopf-

Maier and Kopf, 1987), chemotherapeutic (Wang et al., 2005), radiopharmaceutical (Wang and Meng, 2006), insulin-mimetic (Pessoa et al., 1999) and fungicidal (Eng et al., 1996) activities. Further, tin(IV) complexes characterized by the presence of amino acid ligands have proved to be cytotoxic against the breast adenocarcinoma tumor MCF-7, the colon carcinoma (Gielen, 1996) and hepatocarcinoma HCC Hep G2 cancer (Pellerito et al., 2010). Girasolo et al. (2010) reported the antitumor activity of organotin(IV) complexes containing L-Arginine, N α -t-Boc-L-Arginine and L-Alanyl-L-Arginine against the human colon-rectal carcinoma HT29, observing that for all these complexes, cytotoxic activity was higher than that exerted by cisplatin (Girasolo et al., 2010). Tzimopoulos et al. (2010) reported the results of a screening on wide range of triorganotin aminobenzoates in the K562 myelogenous leukaemia,

*Corresponding author. E-mail: m_monajjemi@yahoo.com.

Table 1. Calculated relative energy (Kcal/mol) and dipole moments (μ in Debye) of the $\text{Sn}(\text{CH}_3)_2(\text{N-acetyl-L-cysteinate})\text{-CNT}$ complex obtained at (LanL2DZ+STO-3G) and (LanL2DZ+6-31G) levels.

Basis set	Gas phase	Water	Methanol	Ethanol
E (Kcal/mol)				
Sto-3G	-1528418.194926134883	-1528361.926661349704	-1528365.446429708648	-1528364.908184099206
6-31G	-1546711.056411545919	-1546663.537831896343	-1546664.499741357760	-1546664.546496487819
μ (Debye)				
Sto-3G	1.9913	24.5881	25.0154	24.9129
6-31G	3.9221	25.2208	25.9544	25.8441

HeLa cervical cancer and HepG2 hepatocellular carcinoma cells, observing that for triorganotin complexes containing aminobenzoates, cytotoxic activity was better than cisplatin and some triorganotin carboxylates drugs (Tzimopoulos et al., 2010). Furthermore, The cytotoxic activity of diorganotin(IV) N-acetyl-L-cysteinate complexes towards human hepatocarcinoma HCC Hep G2 cells were studied (Pellerito et al., 2010). In the case at hand, since the discovery of carbon nanotubes (CNTs) (Iijima, 1991), they have been considered as the ideal material for a variety of applications owing to their unique properties. These properties include their potential biocompatibility in pharmaceutical drug delivery systems and their excellent role as drug carriers with a highly site-selective delivery and sensitivity (Bianco et al., 2005; Mollaamin et al., 2010; Popov et al., 2007; Banerjee et al., 2005; Pastorin et al., 2006; Klumpp et al., 2006; Kostarelos et al., 2007; Raffa et al., 2008; Zhang et al., 2009; Monajjemi et al., 2010; Monajjemi et al., 2009; Monajjemi et al., 2008; Monajjemi et al., 2010). To accelerate the optimal development of CNT as a new effective drug transporter, it is required to better understand the structural properties of the drug-CNT complex. In this paper, we report a computational study of the interaction between diorganotin(IV) complexes of N-acetyl-L-cysteine (H2NAC; (R)-2-acetamido-3-sulfanylpropanoic acid) with CNT. We perform a full geometrical, energetical, nuclear magnetic resonance and vibrational analysis of $\text{Sn}(\text{CH}_3)_2(\text{NAC})\text{-CNT}$ with different basis set to elucidate the effect of site-specific of these systems. The aim of this study was to investigate the stability of $\text{Sn}(\text{CH}_3)_2(\text{N-acetyl-L-cysteinate})\text{-CNT}$ at physiological conditions (temperature, solvent, etc.) and examine the effect of dielectric constant on stability of $\text{Sn}(\text{CH}_3)_2(\text{N-acetyl-L-cysteinate})\text{-CNT}$ complex.

COMPUTATIONAL METHODS

The quantum chemical computations in this work were carried out using Gaussian 98 software package (Frisch et al., 2004). Geometries of $\text{Sn}(\text{CH}_3)_2(\text{N-acetyl-L-cysteinate})\text{-CNT}$ complex were optimized in gas phase using the Hartree-Fock method. We used the STO-3G and 6-31G basis sets for all the atoms except for tin,

for which the LanL2DZ (Mollaamin et al., 2010; Monajjemi et al., 2010; Hay and Wadt, 1985) basis set was used. Moreover, vibrational frequencies were calculated in gas phase on the optimized geometries at the same level of theory to obtain the thermal and enthalpy corrections as well as ΔG , that is, the free energy changes of interaction and entropy at physiological temperature. The gauge including atomic orbital (GIAO) and continuous set of gauge transformations (CSGT) methods (Wrackmeyer, 1985; Ditchfield, 1972; Pulay et al., 1990; Monajjemi et al., 2008; Keith and Bader, 1993) were applied to the optimized structures to achieve anisotropic chemical shift tensor ($\Delta\sigma$) and asymmetry parameter (η). To obtain an estimation of the solvation effects, single point calculations were also conducted on the gas-phase optimized geometries using a self-consistent reaction-field (SCRF) model (Miertus et al., 1981; Miertus and Tomasi, 1982; Monajjemi and Chahkandi, 2005; Monajjemi et al., 2011). Therefore, all calculations were repeated in various solvents, such as water ($\epsilon = 78.39$), methanol ($\epsilon = 32.63$) and ethanol ($\epsilon = 24.55$). It should be noted that according to structure of $\text{Sn}(\text{CH}_3)_2(\text{N-acetyl-L-cysteinate})\text{-CNT}$ complex and number of atoms (86 atoms), our computers are not enough modern to run this heavy molecule. We have not aimed with heavier basis set than 6-31G basis set.

RESULTS AND DISCUSSION

Molecular geometry

The optimized HF/(LanL2DZ+6-31G) structures for the $\text{Sn}(\text{CH}_3)_2(\text{N-acetyl-L-cysteinate})$ and $\text{Sn}(\text{CH}_3)_2(\text{N-acetyl-L-cysteinate})\text{-CNT}$ complex are displayed in Figure 1. Also, Table 1 depicts the calculated relative energy (kcal/mol) and dipole moments (Debye) in gas phase and solvent phases. From Table 1, we can see that with increasing dielectric constant (ϵ) of solvents, the calculated energy of $\text{Sn}(\text{CH}_3)_2(\text{N-acetyl-L-cysteinate})\text{-CNT}$ complex decreases. The plot of μ versus $1/\epsilon$ in both gas phase and in solution is shown in Figure 2. As can be seen from Figure 2, with increasing dielectric constant (ϵ) of solvents, the dipole moment (μ) of $\text{Sn}(\text{CH}_3)_2(\text{N-acetyl-L-cysteinate})\text{-CNT}$ increases.

Calculated NMR parameters

The calculated anisotropic chemical shift tensor ($\Delta\sigma$), total atomic charge and asymmetry parameter (η) for

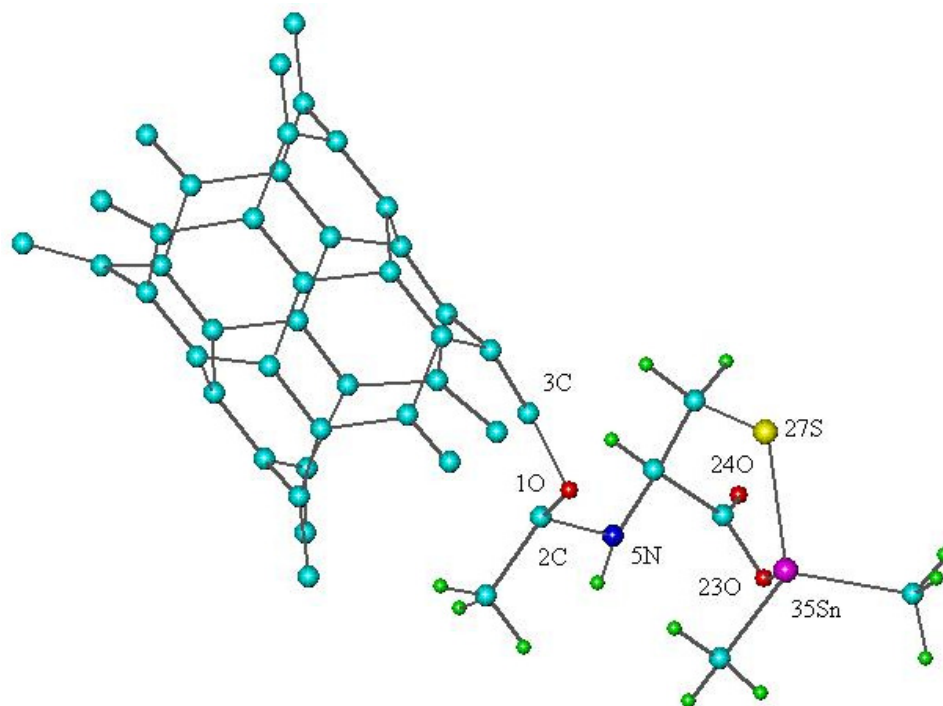


Figure 1. Optimized geometry of the $\text{Sn}(\text{CH}_3)_2(\text{N-acetyl-L-cysteinate})\text{-CNT}$ complex obtained at the (LanL2DZ+6-31G) level.

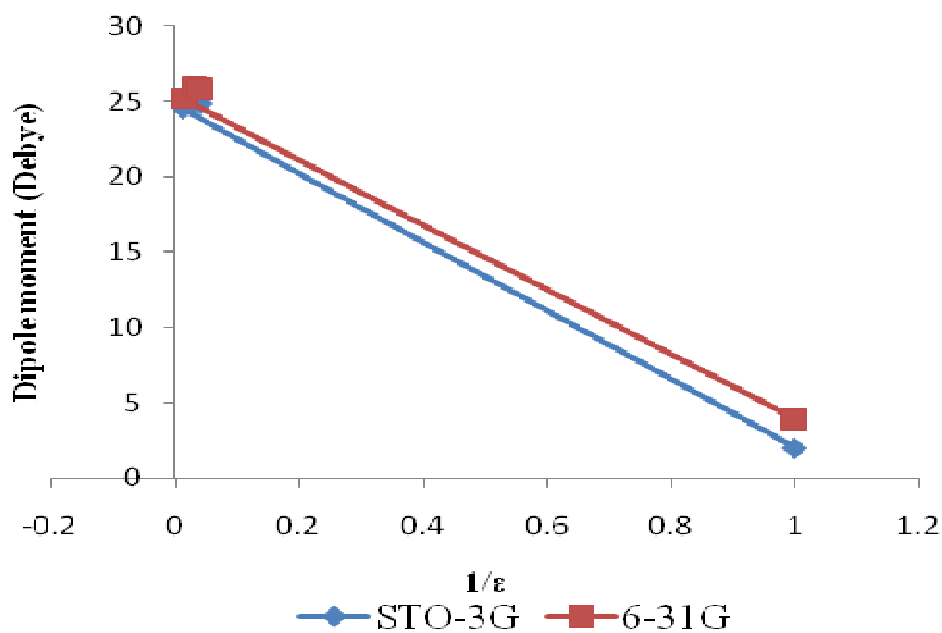


Figure 2. Plot of the μ (Debye) versus the $1/\epsilon$, obtained from the (LanL2DZ+STO-3G) and (LanL2DZ+6-31G) calculations for $\text{Sn}(\text{CH}_3)_2(\text{N-acetyl-L-cysteinate})\text{-CNT}$ complex.

selected atoms of $\text{Sn}(\text{CH}_3)_2(\text{N-acetyl-L-cysteinate})\text{-CNT}$ complex in both gas phase and in solution at GIAO and CSGT methods are specified in Table 2. The graphs of calculated anisotropic chemical shift tensor ($\Delta\sigma$),

asymmetry parameter (η) and total atomic charge versus the atomic number are also drawn in Figure 3a to c, respectively. As shown in Figure 3, the Sn-35 nucleus has maximum total atomic charge and low $\Delta\sigma$ values in

Table 2. Calculated NMR parameters of Sn(CH₃)₂(N-acetyl-L-cysteinate)-CNT complex in gas phase and various solvents at GIAO and CSGT methods.

Atoms	$\Delta\sigma$ (ppm)				η				Charge (a.u.)			
	GIAO		CSGT		GIAO		CSGT		GIAO		CSGT	
	HF/STO-3G	HF/6-31G	HF/STO-3G	HF/6-31G	HF/STO-3G	HF/6-31G	HF/STO-3G	HF/6-31G	HF/STO-3G	HF/6-31G	HF/STO-3G	HF/6-31G
Gas phase												
1O	133.27625	162.2032	151.30455	175.7776	0.76422159395	0.9834975563	0.9300166452	0.9347407944	-0.206606	-0.665951	-0.206606	-0.665951
5N	-57.2367	66.76195	-22.9373	56.26365	0.6262887273	0.3252156915	0.8939214596	0.2662313945	-0.334198	-0.789626	-0.334198	-0.789626
23O	-349.1178	-301.8081	-248.5697	-302.31045	0.3139183965	0.1528865527	0.3507544062	0.1448529152	-0.378221	-0.930993	-0.378221	-0.930993
24O	893.6313	777.985	648.91945	681.3507	0.4924870021	0.3582897897	0.3652486171	0.3748171096	-0.255457	-0.524892	-0.255457	-0.524892
27S	393.09555	153.6641	188.15355	185.67265	0.2234956615	0.3642016438	0.8304278606	0.0889751158	0.036317	-0.174392	0.036317	-0.174392
35Sn	3.307	4.26845	5.98665	5.06225	0.4298090443	0.1535352825	0.6075768585	0.4750800047	0.625426	1.679188	0.625426	1.679188
2C	38.1788	49.1969	20.75265	52.48415	0.4565131126	0.087255586	0.3432501391	0.3628213115	0.238337	0.549121	0.238337	0.549121
3C	-102.699	-126.6157	-105.86055	-134.22655	0.8072211024	0.7654734896	0.7791840303	0.7699297307	0.135517	0.405128	0.135517	0.405128
Water												
1O	-298.01245	-300.86675	-288.25255	-307.59315	0.8861895054	0.8026426653	0.4601752734	0.6260586427	-0.205436	-0.776383	-0.205436	-0.776383
5N	-133.43445	-215.8869	-145.21055	-226.2453	0.0537083938	0.0386257804	0.1667678990	0.1421837271	-0.304099	-0.860286	-0.304099	-0.860286
23O	-207.47025	-222.6352	-181.6076	-230.7312	0.9823661464	0.1573214484	0.5406366640	0.1036517818	-0.369772	-0.919359	-0.369772	-0.919359
24O	909.353	814.2384	694.5349	728.01665	0.4698565062	0.3953785525	0.2887677574	0.3665353921	-0.221098	-0.489641	-0.221098	-0.489641
27S	284.85405	129.7666	-217.006	-163.41745	0.3712559115	0.83366411	0.7676163867	0.9306107949	0.032035	-0.203277	0.032035	-0.203277
35Sn	-4.42025	3.4626	4.5463	3.53725	0.8699267001	0.2932767284	0.7790425286	0.8262657959	0.607104	1.598030	0.607104	1.598030
2C	148.06185	187.45305	122.6329	192.74475	0.2728464489	0.6484607745	0.4392620417	0.4653239582	0.410397	0.914918	0.410397	0.914918
3C	83.1298	-99.01685	77.66165	-103.3895	0.8494241238	0.8790887000	0.9861108965	0.8794843187	0.055560	0.190564	0.055560	0.190564
Methanol												
1O	306.6367	315.3896	-288.51055	-310.52655	0.9104417523	0.8603493679	0.6244042460	0.8928584367	-0.198399	-0.750570	-0.198399	-0.750570
5N	306.6367	315.3896	-288.51055	-310.52655	0.9104417523	0.8603493679	0.6244042460	0.8928584367	-0.198399	-0.750570	-0.198399	-0.750570
23O	-132.8056	-213.95105	-145.5225	-223.4479	0.0363711935	0.0396896953	0.1742039890	0.1449934984	-0.305193	-0.868067	-0.051359	-0.411311
24O	-204.55385	-220.50135	-179.9908	-227.8303	0.9964031467	0.1451753016	0.5623685870	0.1046449638	-0.372293	-0.922565	-0.372293	-0.922565
27S	916.5669	823.7247	701.08365	735.48065	0.4710625050	0.3917073264	0.2935350867	0.3588210892	-0.218476	-0.489386	-0.218476	-0.489386
35Sn	289.6761	129.9141	-222.21485	-161.31185	0.3427158816	0.8774959761	0.7697477845	0.9393674238	0.031227	-0.205365	0.031227	-0.205365
2C	-4.5373	3.61365	4.408	3.58385	0.9161955767	0.3358515628	0.8490148705	0.8536330152	0.603715	1.593134	0.603715	1.593134
3C	146.5689	182.3604	124.0064	189.05055	0.22265091707	0.5901593767	0.3927935948	0.3924688396	0.408575	0.924082	0.408575	0.924082
Ethanol												
1O	307.21795	316.009	-287.6853	-309.91085	0.9031506942	0.8526258978	0.3156621141	0.8997445393	-0.198587	-0.750865	-0.198587	-0.750865
5N	-132.753	-213.9204	-145.47475	-223.45565	0.0403199927	0.0398938109	0.1723692065	0.1429914936	-0.305292	-0.868087	-0.305292	-0.868087
23O	204.0473	-220.72555	-180.20645	-228.24925	0.9989796488	0.1431929508	0.5601834895	0.1014187119	-0.372438	-0.922664	-0.372438	-0.922664

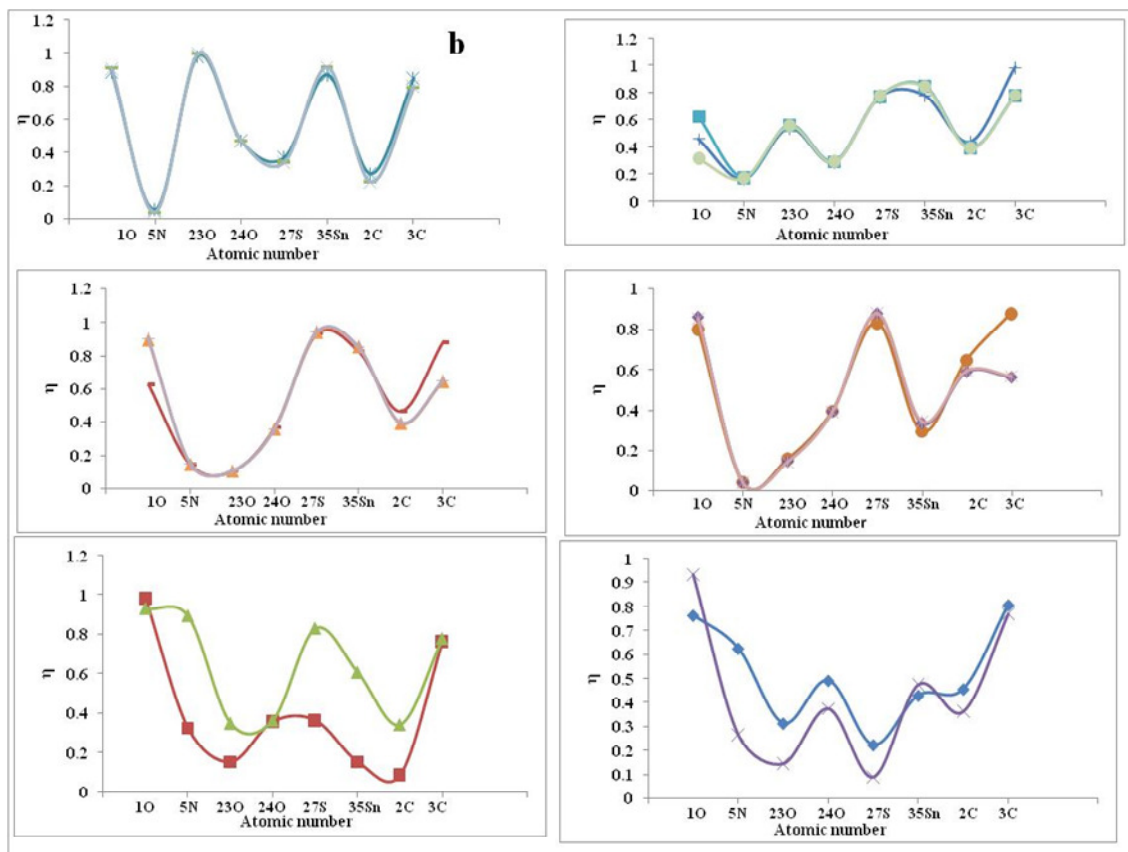
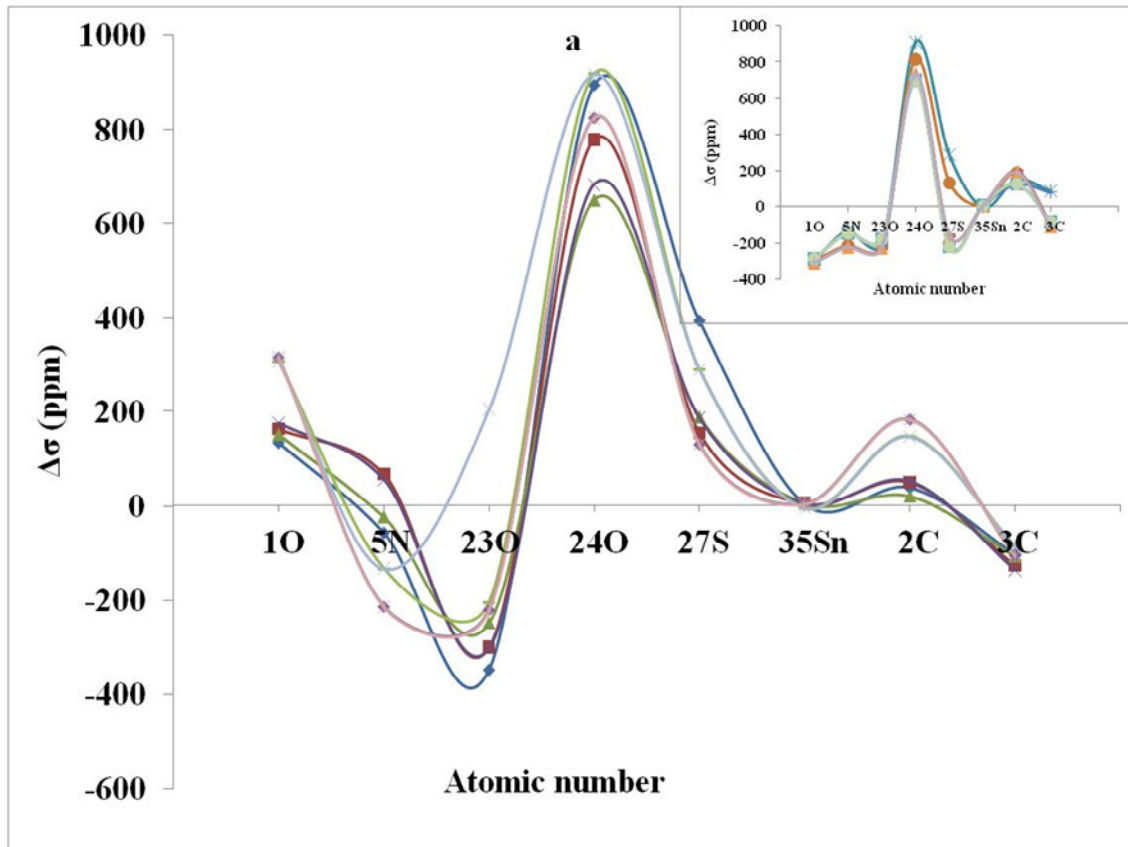
Table 2. cont

24O	916.32285	823.794	701.02135	735.5615	0.4701214751	0.3901241086	0.2919841676	0.3569444809	-0.218414	-0.489307	-0.218414	-0.489307
27S	290.08825	129.9081	-221.7231	-161.15845	0.3402769087	0.8765896814	0.7764441323	0.9438332449	0.031256	-0.204437	0.031256	-0.204437
35Sn	-4.55265	3.6277	4.40665	3.5843	0.9132812757	0.3427744469	0.8460700548	0.8492634750	0.603779	1.593023	0.603779	1.593023
2C	146.43065	182.46825	123.8593	189.1353	0.2224914054	0.5933199337	0.3917968243	0.3946460549	0.408701	0.923818	0.408701	0.923818
3C	-85.53375	-105.47775	-85.16655	-111.64375	0.7982480599	0.5675903211	0.7803715190	0.6458768870	0.038610	0.176795	0.038610	0.176795

both gas phase and in solution, meaning the relative chemical shift at the site of Sn-35 is predominantly governed by local diamagnetic shielding term (σ^d). Further, Tin atom has large amounts of asymmetry parameter (η) in both gas phase and in solution (Figure 3b). The results in solution indicate that the anisotropic chemical shift tensor ($\Delta\sigma$) of Sn-35 decreases in the order, gas phase > ethanol > methanol > water, and also asymmetry parameter (η) at the site of Sn-35 decreases in the order, ethanol > methanol > water > gas phase (Figure 3a and b). The observed changes can be due to the presence of the solvent molecule in the tin inner coordination sphere. Since sulfur atom possess negative and tin atom has positive charges (Figure 3c), this difference in the charges leads to a larger anisotropic chemical shift tensor ($\Delta\sigma$) for the sulfur atom (Figure 3a). The results in Figure 3a show that, with increase of dielectric constant from gas phase to water, the $\Delta\sigma$ at the site of sulfur atom decreases. In addition, Figure 3b indicates that asymmetry parameter (η) of S-27 in solution are larger than gas phase. The observed effect is probably due to the nonspecific solute-solvent interaction (such as polarisability/polarity) at the site of S-27 nucleus. Since N-5 is more negative than S-27 (Figure 3c), N-5 nucleus has the lower $\Delta\sigma$ value than the S-27 nucleus (Figure 3a). Also, Figure 3b shows that η for N-5 has minimum value. The results in the solution show that with increasing dielectric constant of solvent, the $\Delta\sigma$ and η values of N-5 atom decrease (Figure 3a and

b). It can be said that the NMR ($\Delta\sigma$, η) parameters at the site of N-5 nucleus are significantly influenced by intermolecular hydrogen-bonding interactions. Since carbon atoms (C-2 and C-3) are more positive than N-5 (Figure 3c), the $\Delta\sigma$ values at the sites of C-2 and C-3 are greater than the N-5 nucleus (Figure 3a). As shown in Figure 3b, the η values for the carbon atoms are larger than nitrogen atom. The results in solution show that with increasing dielectric constant of solvent, the $\Delta\sigma$ and η values of C-2 atom increase (Figure 3a and b). Moreover, with increasing dielectric constant of solvent, the $\Delta\sigma$ value at the site of C-3 increases (Figure 3a). The observed effect is probably due to the intermolecular hydrogen-bonding interactions at the sites of carbon nuclei. The results in Figure 3b indicate that the η values of C-3 are larger than that of C-2. Also, since the $\Delta\sigma$ constants for the C-2 are larger than $\Delta\sigma$ values for the C-3 (Figure 3a), it seems that the C-3 is more shielded than the C-2 nucleus. Since the electrostatic properties are mainly dependent on the electronic densities at the sites of nuclei, oxygen plays a significantly different role among the other nuclei (S, C, Sn and N atoms). Total atomic charge for O-23 nucleus is minimum, meaning O-23 nucleus has maximum electron shielding (Figure 3c). This leads to a minimum anisotropic chemical shift tensor ($\Delta\sigma$) at the site of O-23 atom (Figure 3a). Also, Figure 3b shows that O-23 has small amounts of η in both gas phase and solution. The results in Figure 3a indicate that, the anisotropic chemical shift tensor ($\Delta\sigma$) at

the site of O-23 decreases in the order methanol > ethanol > water > gas phase. Meaning O-23 nucleus has maximum electron shielding in gas phase, but the quantity is minimum in methanol. In addition, Figure 3b indicates that asymmetry parameter (η) of O-23 in the solution are larger than gas phase. In this regard, it seems that the NMR ($\Delta\sigma$, η) parameters at the site of O-23 nucleus are significantly influenced by intermolecular hydrogen-bonding interactions. On the other hand, Figure 3c shows that O-23 possess more negative than O-24 nucleus. This difference in the total atomic charge values lead to a maximum anisotropic chemical shift tensor ($\Delta\sigma$) at the site of O-24 atom (Figure 3a). The results in the solution indicate that the anisotropic chemical shift tensor ($\Delta\sigma$) of O-24 decreases in the order ethanol > methanol > water > gas phase. Meaning O-24 nucleus has maximum electron shielding in gas phase, but the quantity is minimum in methanol. In addition, Figure 3b indicates that asymmetry parameter (η) of O-24 in gas phase are larger than solution. It can be said that the NMR ($\Delta\sigma$, η) parameters at the site of O-24 nucleus are significantly influenced by intermolecular hydrogen-bonding interactions. As shown in Figure 3b, O-1 nucleus has large amounts of anisotropic chemical shift tensor ($\Delta\sigma$) in gas phase, but the quantity is smaller in methanol. Moreover, with increase of dielectric constant from gas phase to water, the asymmetry parameter (η) at the site of O-1 decreases (Figure 3b). The observed effect is probably due to the



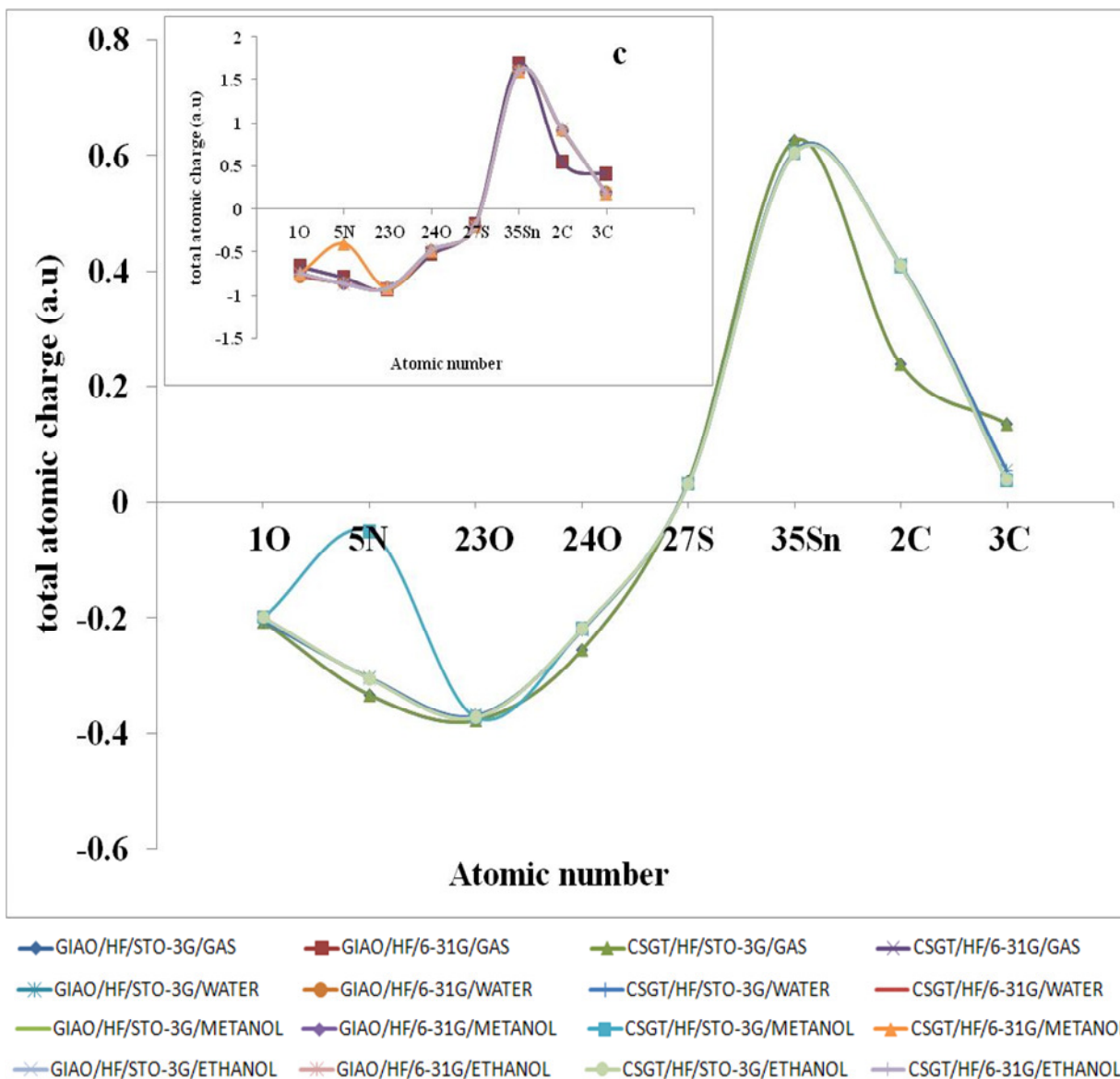


Figure 3. Graphs of the $\Delta\sigma$ (ppm) versus atomic number: (a) η versus atomic number; (b) total atomic charge (a.u) versus atomic number; (c) for selected atoms of $\text{Sn}(\text{CH}_3)_2(\text{N-acetyl-L-cysteinate})\text{-CNT}$ complex in both gas phase and in solution obtain from the GIAO and CSGT methods.

intermolecular hydrogen-bonding interactions at the site of O-1 nucleus.

Thermodynamic analysis

Table 3 displays the calculated relative energies (ΔE), enthalpies (ΔH) and free Gibbs energies (ΔG) as well as entropy (ΔS) in both gas phase and in solution, for $\text{Sn}(\text{CH}_3)_2(\text{NAC})\text{-CNT}$ complex at the physiological temperature. In addition, the plots of calculated relative energies (ΔE), enthalpies (ΔH) and entropy (ΔS) as well as free Gibbs energies (ΔG) versus the physiological temperature are drawn in Figure 4a to d, respectively.

From Table 3 and Figure 4, it can be seen that $\text{Sn}(\text{CH}_3)_2(\text{N-acetyl-L-cysteinate})\text{-CNT}$ complex has negative values of relative energies (ΔE), enthalpies (ΔH) and free Gibbs energies (ΔG) in both gas phase and in solution. Also, our results in Table 3 and Figure 4c show that entropy (ΔS) for $\text{Sn}(\text{CH}_3)_2(\text{N-acetyl-L-cysteinate})\text{-CNT}$ system has positive values. These observations can be related to the structural stability of the $\text{Sn}(\text{CH}_3)_2(\text{N-acetyl-L-cysteinate})\text{-CNT}$ in both gas phase and in solution.

The results in Figure 4 show that, with increase of dielectric constant from gas phase to water, the stability of $\text{Sn}(\text{CH}_3)_2(\text{N-acetyl-L-cysteinate})\text{-CNT}$ complex decreases.

Table 3. Calculated relative electronic energies (Kcal/mol), enthalpies (Kcal/mol), free Gibbs energies (Kcal/mol) and entropies (Kcal/molK) in both gas phase and in solution, for the Sn(CH₃)₂(N-acetyl-L-cysteinate)-CNT complex obtained at the level of HF/(LanL2DZ+STO-3G).

Temperature (K)	Gas phase	Water	Ethanol	Methanol
ΔE (Kcal/mol)				
298.15	-1528088.69709835099	-1528012.26240660171	-1528015.4118361785	-1528015.2235857555
300.15	-1528088.40091768547	-1528011.96308842914	-1528015.10938049888	-1528014.92050257447
302.15	-1528088.10285451572	-1528011.66188775234	-1528014.80441481362	-1528014.61616439062
304.15	-1528087.80290884174	-1528011.35943207272	-1528014.49882162695	-1528014.31057120395
306.15	-1528087.50170816494	-1528011.05572139028	-1528014.19134593605	-1528014.00309551305
308.15	-1528087.19925248532	-1528010.75012820361	-1528013.88198774092	-1528013.69373731792
310.15	-1528086.89491430147	-1528010.44265251271	-1528013.57137454297	-1528013.38312411997
312.15	-1528086.5893211148	-1528010.13392181899	-1528013.2595063422	-1528013.0712559192
313.15	-1528086.43558326935	-1528009.97892897072	-1528013.1026309897	-1528012.9143805667
ΔH (Kcal/mol)				
298.15	-1528088.10473701995	-1528011.66941776926	-1528014.81947484746	-1528014.63122442446
300.15	-1528087.80416384456	-1528011.36633458823	-1528014.51262665797	-1528014.32437623497
302.15	-1528087.50233566635	-1528011.06136890297	-1528014.20452346566	-1528014.01627304266
304.15	-1528087.19862498391	-1528010.75514821489	-1528013.89453776912	-1528013.70628734612
306.15	-1528086.89365929865	-1528010.44704502258	-1528013.58266956835	-1528013.39441914535
308.15	-1528086.58681110916	-1528010.13768682745	-1528013.27017386617	-1528013.08192344317
310.15	-1528086.27870791685	-1528009.82644612809	-1528012.95516815835	-1528012.76691773535
312.15	-1528085.96872222031	-1528009.51395042591	-1528012.63890744771	-1528012.45128452612
313.15	-1528085.81310187063	-1528009.35707507341	-1528012.48077709239	-1528012.29252666939
ΔG (Kcal/mol)				
298.15	-1528156.53313827904	-1528084.24372084422	-1528087.32287026309	-1528086.34020305503
300.15	-1528156.99309681257	-1528084.7319169412	-1528087.80981135725	-1528086.82212413791
302.15	-1528157.45493785033	-1528085.221368041	-1528088.29926245705	-1528087.30655522643
304.15	-1528157.91866139232	-1528085.71332914644	-1528088.79059606108	-1528087.79224131777
306.15	-1528158.38489493995	-1528086.20717275611	-1528089.28443967075	-1528088.28043741475
308.15	-1528158.85301099181	-1528086.70352637142	-1528089.78016578465	-1528088.77114351737
310.15	-1528159.3230095479	-1528087.20113498955	-1528090.27777440278	-1528089.26310462281
312.15	-1528159.79489060822	-1528087.70125361332	-1528090.77726552514	-1528089.75757573389
313.15	-1528160.0320861412	-1528087.95162667591	-1528097.5783248473	-1528090.00543879084
ΔS (Kcal/mol)				
298.15	0.229512	0.243418	0.24318	0.240517
300.15	0.230516	0.244432	0.244206	0.241542
302.15	0.231519	0.245444	0.24523	0.242566
304.15	0.23252	0.246455	0.246252	0.243588
306.15	0.23352	0.247464	0.247272	0.244609
308.15	0.234519	0.248472	0.248292	0.245628
310.15	0.235516	0.249479	0.249309	0.246645
312.15	0.236512	0.250483	0.250325	0.247661
313.15	0.237009	0.250985	0.250833	0.248169

Conclusion

1. O-24 has maximum anisotropic chemical shift tensor ($\Delta\sigma$) constant, but the quantity in the O-23 and O-1 nuclei are minimum.

2. Sn-35 has maximum total atomic charge, but the quantity in the O-23 nucleus is minimum.

3. The NMR ($\Delta\sigma$, η) parameters at the sites of nitrogen, oxygen as well as C-2 and C-3 are significantly influenced by intermolecular hydrogen-bonding interactions,

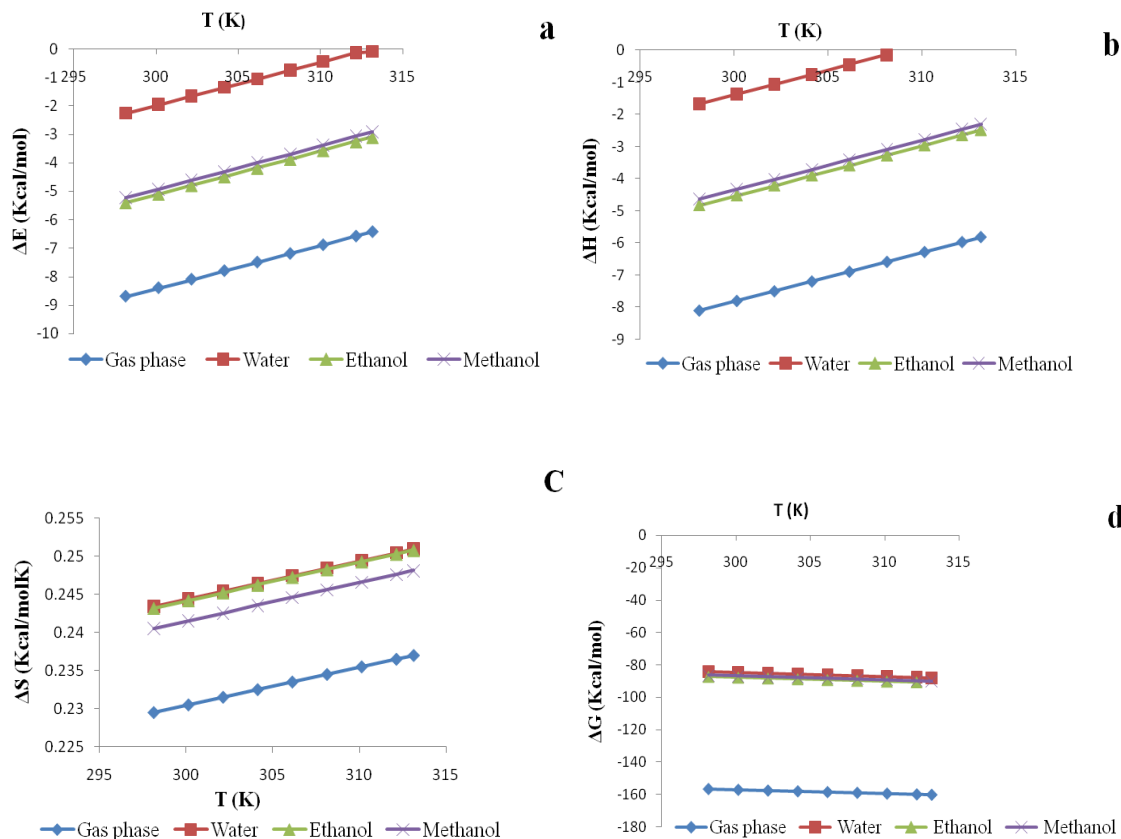


Figure 4. Plots of the ΔE (Kcal/mol) versus the T (K): (a) ΔH (Kcal/mol) versus the T (K); (b) ΔS (Kcal/molK) versus the T (K); (c) ΔG (Kcal/mol) versus the T (K); (d) for $\text{Sn}(\text{CH}_3)_2(\text{N-acetyl-L-cysteinate})\text{-CNT}$ complex in both gas phase and in solution, obtained from the (LanL2DZ+STO-3G) calculations .

interactions, but the quantity at the site of S-27 is influenced by nonspecific solute-solvent interaction, such as polarisability/polarity.

4. The thermodynamic analysis shows that with increase of dielectric constant from gas phase to water, the stability of $\text{Sn}(\text{CH}_3)_2(\text{N-acetyl-L-cysteinate})\text{-CNT}$ complex decreases.

REFERENCES

- Banerjee S, Hemraj-Benny T, Wong SS (2005). Covalent surface chemistry of singlewalled carbon nanotubes. *Adv. Mater.*, 17: 17–29.
- Bianco A, Kostarelos K, Partidos CD, Prato M (2005). Biomedical applications of functionalised carbon nanotubes. *Chem. Commun.*, pp. 571-577.
- Clarke MJ, Zhu F, Frasca DR (1999). Non-platinum chemotherapeutic metallopharmaceuticals. *Chem. Rev.*, 99: 2511-2534.
- Ditchfield R (1972). Molecular-orbital theory of magnetic shielding and magnetic susceptibility. *J. Chem. Phys.*, 56: 5688-5692.
- Eng G, Whalen D, Zhang YZ, Kirksey A, Otieno M, Khoo LE, James BD (1996). The monomeric SubPc has a λ max value of 560 nm, whereas the dinuclear. *Appl. Organomet. Chem.*, 10 (7): 501-503.
- Frisch MJ, Trucks GW, Schlegel HB, Scuseria GE, Robb MA, Cheeseman JR, Zakrzewski VG, Montgomery JA Jr, Stratmann RE, Burant JC, Dapprich S, Millam JM, Daniels AD, Kudin KN, Strain MC, Farkas O, Tomasi J, Barone V, Cossi M, Cammi R, Mennucci B, Pomelli C, Adamo C, Clifford S, Ochterski J, Petersson GA, Ayala PY, Cui Q, Morokuma K, Malick DK, Rabuck AD, Raghavachari K, Raghavachari JB, Cioslowski J, Ortiz JV, Baboul AG, Stefanov BB, Liu G, Liashenko A, Piskorz P, Komaromi I, Gomperts R, Martin RL, Fox DJ, Keith T, Al-Laham MA, Peng CY, Nanayakkara A, Gonzalez C, Challacombe M, Gill PMW, Johnson B, Chen W, Wong MW, Andres JL, Gonzalez C, Head-Gordon M, Replogle ES, Pople JA (1998). Gaussian 98 Revision A.7. Gaussian, Inc., Pittsburgh.
- Gielen M (1996). Tin-Based Antitumor Drugs. *Coord. Chem. Rev.*, 151: 41-51.
- Girasolo MA, Rubino S, Portanova P, Calvaruso G, Stocco G, Ruisi G (2010). Novel diorganotin(IV) derivatives of L-Arginine (HArg), Na-(tert-Butoxycarbonyl)-L. *J. Organom. Chem.*, 695: 609-618.
- Goldberg DE, Sharma V, Oksman A, Gluzman I, Welles TE, Piwnica-Worms D (1997). Probing the metal(III) coordination complexes. *J. Biol. Chem.*, 272(10): 6567-6572.
- Hay PJ, Wadt WR (1985). Ab initio effective core Potentials for the transition metal atoms Sc to Hg. *J. Chem. Phys.*, 82: 270-270.
- Iijima S (1991). Helical microtubules of graphitic carbon, *Nature*, 354: 56-58.
- Keith TA, Bader RFW (1993). Calculation of Magnetic Response. *Chem. Phys. Lett.*, 210: 223-223.
- Klumpp C, Kostarelos K, Prato M, Bianco A (2006). Functionalized carbon nanotubes as emerging nanovectors for the delivery of therapeutics, *Biochim. Biophys. Acta. Biomembr.*, 1758: 404-412.
- Kostarelos K, Lacerda L, Pastorin G (2007). Cellular uptake of functionalized carbon nanotubes is independent of functional group and cell type. *Nat. Nanotechnol.*, 2: 108-113.
- Köpf-Maier P, Köpf H (1987). Anti-HIV Effects of Gramicidin in vitro. *Chem. Rev.*, 87 (5): 1137-1152.
- Miertus M, Scrocco E, Tomasi J (1981). From Theozymes to Artificial

- Enzymes: Enzyme-Like Receptors . Chem. Chem. Phys., 55: 117-129.
- Miertus S, Tomasi J (1982). Approximate evaluations of the electrostatic free energy and internal changes in solution. Phys., 65: 239-252.
- Mollaamin F, Layali I, Ilkhani A R, Monajjemi M (2010). Nanomolecular simulation of the voltage-gated potassium channel protein by gyration radius study. Afr. J. Microbiol. Res., 4(24): 2795-2803.
- Mollaamin F, Shahani poor K, Nejadstattari T, Monajjemi M (2010). Bio-nanomodelling of active site in oxidized azurin using by computational methods. Afr. J. Microbiol. Res., 4(20): 2098-2108.
- Mollaamin F, Varmaghani Z, Monajjemi M (2011). Dielectric effect on thermodynamic properties in vinblastine by DFT/Onsager modeling. Phys. Chem. Liquids, 49(3): 318-336.
- Monajjemi M, Chahkandi B (2005). Theoretical investigation of hydrogen bonding in Watson-Crick, Hoogestein and their reversed and other models: comparison and analysis for configurations of adenine-thymine base pairs in 9 models. J. Molecular Struct. Theochem., 714(1): 43-60 JAN 31.
- Monajjemi M, Afsharnezhad S, Jaafari MR, Mirdamadi S, Mollaamin F, Monajemi H (2008). Investigation of energy and NMR isotropic shift on the internal rotation Barrier of Θ_4 dihedral angle of DLPC. A GIAO study Chem., 17(1):55-69.
- Monajjemi M, Mahdavian L, Mollaamin F (2008). Characterization of nanocrystalline cylicon germanium film and nanotube in adsorption gas by monte carlo and langevin dynamic simulation Bull. Chem. Soc. Ethiop., 22(2): 1-10.
- Monajjemi M, Mahdavian L, Mollaamin F, Khaleghian M (2009). Interaction of Na, Mg, Al, Si with Carbon Nanotube (CNT):NMR and IR Study. Russian J. Inorganic Chem., 54(9): 1465-1473.
- Monajjemi M, Baie M T, Mollaamin F (2010). Interaction between threonine and cadmium cation in $[\text{Cd}(\text{Thr})_n]^{2+}$ ($n = 1-3$) complexes: density functional calculations. Russian Chemical Bulletin. 59(5): 886-889.
- Monajjemi M, Lee VS, Khaleghian M, Honarparvar B, Mollaamin F (2010). Theoretical Description of Electromagnetic Nonbonded Interactions of Radical, Cationic, and Anionic NH_2 BHNBNH 2 Inside of the B 18 N18 Nanoring. J. Phys. Chem. C. 114: 15315-15330.
- Monajjemi M, Saedi L, Najafi F, Mollaamin F (2010). Physical properties of active site of tubulin-binding as anticancer nanotechnology investigation. Int. J. Phys. Sci., 5(10): 1609-1621.
- Nath M, Pokharia S, Yadav R (2001). Calix[4]arenes as Molecular Platforms in Magnetic Resonance Imagery. Coord. Chem. Rev., 215: 99-149 and references therein.
- Pastorin G, Wu W, Wieckowski SB, Briand J-P, Kostarelos K, Prato M, (2006). Double functionalisation of carbon nanotubes for multimodal drug delivery. Chem. Commun., pp. 1182-1184.
- Pellerito L, Prinziavalli C, Casella G, Fiore T, Pellerito O, Giuliano M, Scopelliti M, Pellerito C (2010). Diorganotin(IV) N-acetyl-L-cysteinate complexes: synthesis. J. Inorg. Biochem. 104: 750-758.
- Pessoa JC, Covaco I, Correia I, Duarte MT, Gillard R D, Henriques RT, Higes FJ, Madeira C, Tomaz I (1999). Preparation and ... derived from amino acids and aromatic o-hydroxyaldehydes. Inorg. Chim. Acta, 293 (1): 1-11.
- Plesch G, Friebel C, Svajlenova O, Kratsmar-Smogrovic J, Mlynarcik D (1988). Copper(II) complexes of the general composition $\text{Cu}(\text{ligand})_2\text{X}_2$ (where $\text{X}=\text{Cl}^-$, Br. Inorg. Chim. Acta, 151 (2): 139-143.
- Popov AM, Lozovik YE, Fiorito S, Yahia LH (2007). Biocompatibility and applications of carbon nanotubes in medical nanorobots. Int. J. Nanomed., 2: 361-372.
- Pulay P, Wolinski K, Hinton JF (1990). The 3-21+G basis set for first-row elements. J. Am. Chem. Soc. 112: 8251-8260.
- Raffa V, Ciofani G, Nitodas S, Karachalios T, D'Alessandro D, Masini M (2008). Can the properties of carbon nanotubes influence their internalization by living cells? Carbon. 46: 1600-1610.
- Tzimopoulos D, Sanidas I, Varvogli AC, Czapik A, Gdaniec M, Nikolakaki E, Akrivos PD (2010). Detection of elevated antibodies against SR. J. Inorg. Biochem. 104: 423-430.
- Wadt WR, Hay PJ (1985). DeMon2k. J. Chem. Phys., 82: 284-284.
- Wang MZ, Meng Z, Liu B, Cai G, Zhang C, Wang X (2005). Effects of extrusion and a Magnesium Lattice. Inorg. Chem. Commun., 8(4): 368-371.
- Wang MZ, Meng Z (2006). Determine the effects of acupuncture on specific clinical symptoms in ... Acupuncture for the Prevention of Radiation-Induced Xerostomia. J. Fu, Appl. Radiat. Isot. 64 (2): 235-240.
- Wrackmeyer B (1985). A multinuclear NMR study unambiguously confirmed that metal tetraolates retain their polynuclear structure in solution. Annu. Rep. NMR Spectrosc., 16: 73-186.
- Zhang X, Meng L, Lu Q, Fei Z, Dyson PJ (2009). Targeted delivery and controlled release of doxorubicin to cancer cells using modified single wall carbon nanotubes. Biomaterials. 30: 6041-6047.